Synthesis of High-Purity Phthalocyanines (pc): High Intrinsic Conductivities in the Molecular Conductors H_2(pc)I and Ni(pc)I

Julia A. Thompson, Kazuhiko Murata, Douglas C. Miller, Judith L. Stanton, William E. Broderick,† Brian M. Hoffman,* and James A. Ibers*

Department of Chemistry and Materials Research Center, Northwestern University, Evanston, Illinois 60208-3113

Received April 29, 1993

We show that one can prepare M(pc)I crystals, M = "H_2" and Ni, with remarkably improved charge-transport properties by carefully avoiding impurities in the preparation of the M(pc) *precursors*. The purest H_2(pc) (<60 ppm free-radical impurities) was prepared by a melt method in quartz and Teflon vessels while very pure Ni(pc) (170–250 ppm) could *only* be obtained by metalation of the pure H_2(pc). Template syntheses of Ni(pc) result in impure material and are to be discouraged for applications requiring very pure M(pc) materials. H_2(pc)I and Ni(pc)I synthesized from the high-purity precursors remain metallic down to ca. 3 K, a far lower temperature than ever before observed. At this temperature the conductivities exhibit maximum values that are ca. 30-fold greater than at room temperature, not 5–7-fold as seen before, with absolute values of $\sigma \sim (1\text{–}2) \times 10^4\ \Omega^{-1}\ cm^{-1}$. The study of a series of Ni(pc)I compounds prepared from Ni(pc) parent materials exhibiting a range of purity levels further shows a strong correlation between the charge-transport properties and the level of paramagnetic impurities in the macrocycle precursor. However, the maximum conductivity appears to saturate at the lowest impurity concentrations, which suggests that the behavior exhibited by the best materials prepared are representative for the first time of the limiting, *intrinsic* charge-transport properties of H_2(pc)I and Ni(pc)I. A full structure report for H_2(pc)I–1 is presented also. The structure consists of metal-over-metal stacks of partially oxidized H_2(pc) groups surrounded by linear chains of triiodide anions. The two H_2(pc) molecules within a unit cell are staggered by 40°. H_2(pc)I crystallizes with two formula units in the tetragonal space group D^2_{4h} – $P4/mcc$ with a = 13.931(2) Å, c = 6.411(1) Å, and V = 1244.2(6) Å^3 (T = 108 K).

Introduction

Since their discovery over 60 years ago,[1–4] metallophthalocyanines (M(pc), M = "H_2", Ni, Cu, ...) have been of wide interest, in part because of their applications in coloration, photochemistry, catalysis, and imaging.[5,6] Historically, it has been difficult to purify metallophthalocyanines.[7] Literature reports affirm that M(pc) compounds obtained commercially typically are not very pure and that the impurities vary with supplier and batch.[8] Sublimation can reduce the level of some organic impurities, but it cannot reliably remove an M′(pc) impurity. Other types of purification, such as recrystallization from concentrated H_2SO_4, may actually increase the level of M′(pc) contaminants where M′ is a transition metal ion.[9] Nonetheless, attempts to purify M(pc) materials have improved the photosensitivity of VO(pc) by 100%[8] and the electrical gas sensing properties of Zn(pc).[10] We have now devised procedures for synthesizing M(pc) (M = H_2, Ni) with greatly reduced levels of paramagnetic impurities and have applied them to the study of M(pc)-based quasi-one-dimensional conductors.[11–27] We show that the use of the newly prepared M(pc) precursors leads to a remarkable improvement in the charge-transport properties of the M(pc)I conductors, M = "H_2" and Ni, whose crystals consist of metal-over-metal stacks of partially oxidized M(pc) units surrounded by I_3^- chains.[13,14,16–19,28]

Low-dimensional molecular metals are of interest because of their tendency to exhibit instabilities, such as lattice distortions

† Present address: Department of Chemistry, State University of New York at Albany, Albany, NY 12222.

(1) Kasuga, K.; Tsutsui, M. *Coord. Chem. Rev.* **1980**, *32*, 67–95.
(2) Linstead, R. P. *J. Chem. Soc.* **1934**, 1016–1017.
(3) Barrett, P. A.; Dent, C. E.; Linstead, R. P. *J. Chem. Soc.* **1936**, 1719–1736.
(4) Braun, A.; Tcherniac, J. *Ber. Dtsch. Chem. Ges.* **1907**, *40*, 2709–2714.
(5) Moser, F. H.; Thomas, A. L. *The Phthalocyanines*; CRC Press: Boca Raton, FL, 1983; Vol. 1–2.
(6) *Phthalocyanines: Properties and Applications*; Leznoff, C. C., Lever, A. B. P., Eds.; VCH Publishers: New York, 1989.
(7) Leznoff, C. C. In *Phthalocyanines: Properties and Applications*; Leznoff, C. C., Lever, A. B. P., Eds.; VCH Publishers: New York, 1989; pp 20–23.
(8) Wagner, H. J.; Loutfy, R. O.; Hsiao, C.-K. *J. Mater. Sci.* **1982**, *17*, 2781–2791.
(9) Loutfy, R. O.; Hsiao, C.-K. *Can. J. Chem.* **1979**, *57*, 2546–2548.
(10) Collins, R. A.; Mohammed, K. A. *Thin Solid Films* **1986**, *145*, 133–145.
(11) Hoffman, B. M.; Ibers, J. A. *Acc. Chem. Res.* **1983**, *16*, 15–21.
(12) Palmer, S. M.; Stanton, J. L.; Martinsen, J.; Ogawa, M. Y.; Heuer, W. B.; Van Wallendael, S. E.; Hoffman, B. M.; Ibers, J. A. *Mol. Cryst. Liq. Cryst.* **1985**, *125*, 1–11.
(13) Marks, T. J. *Science* **1985**, *227*, 881–889.
(14) Marks, T. J. *Angew. Chem., Int. Ed. Engl.* **1990**, *29*, 857–879.
(15) Hanack, M. *Mol. Cryst. Liq. Cryst.* **1988**, *160*, 133–137.
(16) Martinsen, J.; Palmer, S. M.; Tanaka, J.; Greene, R. C.; Hoffman, B. M. *Phys. Rev. B: Condens. Matter* **1984**, *30*, 6269–6276.
(17) Schramm, C. J.; Scaringe, R. P.; Stojakovic, D. R.; Hoffman, B. M.; Ibers, J. A.; Marks, T. J. *J. Am. Chem. Soc.* **1980**, *102*, 6702–6713.
(18) Inabe, T.; Marks, T. J.; Burton, R. L.; Lyding, J. W.; McCarthy, W. J.; Kannewurf, C. R.; Reisner, G. M.; Herbstein, F. H. *Solid State Commun.* **1985**, *54*, 501–504.
(19) Inabe, T.; Marks, T. J.; Lyding, J. W.; Burton, R.; Kannewurf, C. R. *Mol. Cryst. Liq. Cryst.* **1985**, *118*, 353–356.
(20) Ogawa, M. Y.; Martinsen, J.; Palmer, S. M.; Stanton, J. L.; Tanaka, J.; Greene, R. L.; Hoffman, B. M.; Ibers, J. A. *J. Am. Chem. Soc.* **1987**, *109*, 1115–1121.
(21) Martinsen, J.; Stanton, J. L.; Greene, R. L.; Tanaka, J.; Hoffman, B. M.; Ibers, J. A. *J. Am. Chem. Soc.* **1985**, *107*, 6915–6920.
(22) Palmer, S. M.; Stanton, J. L.; Jaggi, N. K.; Hoffman, B. M.; Ibers, J. A.; Schwartz, L. H. *Inorg. Chem.* **1985**, *24*, 2040–2046.
(23) Almeida, M.; Kanatzidis, M. G.; Tonge, L. M.; Marks, T. J.; Marcy, H. O.; McCarthy, W. J.; Kannewurf, C. R. *Solid State Commun.* **1987**, *63*, 457–461.
(24) Yakushi, K.; Yamakado, H.; Yoshitake, M.; Kosugi, N.; Kuroda, H.; Sugano, T.; Kinoshita, M.; Kawamoto, A.; Tanaka, J. *Bull. Chem. Soc. Jpn.* **1989**, *62*, 687–696.
(25) Yamakado, H.; Yakushi, K.; Kosugi, N.; Kuroda, H.; Kawamoto, A.; Tanaka, J.; Sugano, T.; Kinoshita, M.; Hino, S. *Bull. Chem. Soc. Jpn.* **1989**, *62*, 2267–2272.
(26) Futamata, M. *Mol. Cryst. Liq. Cryst.* **1991**, *197*, 109–120.
(27) Futamata, M.; Takaki, Y. *Synth. Met.* **1991**, *39*, 343–353.
(28) Schramm, C. J. Ph.D. Thesis, Northwestern University, 1979.

0020-1669/93/1332-3546$04.00/0

(Peierls transition), spin-density-wave formation, and anion ordering, that cause these materials to become insulators.[29-31] The M(pc)I materials give every indication of being highly one-dimensional[14,16,18,20] and typically have shown a conductivity maximum reminiscent of a Peierls transition. However, two of these compounds, Ni(pc)I and H_2(pc)I, exhibit conductivity maxima with $\sigma_{rel}^{max} = \sigma_{max}/\sigma_{RT} \sim 5$–7 at $T = 25$ and 15 K, respectively, yet remain conducting down to the lowest temperature measured, 50 mK[16] and 1.5 K.[18] In fact Ni(pc)I is the first molecular conductor without a chalcogen atom whose conductivity does not appear to vanish as $T \rightarrow 0$ K.[16] We now report that even these conductivities were strongly limited by impurities. H_2(pc)I and Ni(pc)I synthesized from high-purity precursors remain metallic down to ca. 3 K, a far lower temperature than ever before observed. At this temperature the conductivities exhibit maximum values that are ca. 30-fold greater than at room temperature, *not* 5–7-fold, with absolute values of $\sigma \sim (1\text{–}2) \times 10^4\ \Omega^{-1}\ cm^{-1}$. The study of a series of Ni(pc)I compounds prepared from Ni(pc) parent materials exhibiting a range of purity levels further shows a strong correlation between the charge-transport properties and the level of paramagnetic impurities in the macrocycle precursor. However, the maximum conductivity appears to saturate at the lowest impurity concentrations, which suggests that the behaviors exhibited by the best materials prepared are representative for the first time of the limiting, *intrinsic* charge-transport properties of H_2(pc)I and Ni(pc)I. Such improvements may well be realized in other applications of M(pc) compounds.

Experimental Section

Phthalonitrile and hydroquinone (Aldrich) were purified prior to use by recrystallization from ethanol and by sublimation, respectively. The solvents 1-chloronaphthalene and quinoline (Fluka) were distilled under vacuum.

Synthesis of H_2(pc). Three different types of H_2(pc) were employed; they are labeled H_2(pc)–*i*, $i = 1$–3. Within error, each preparation gave the same satisfactory elemental analysis. H_2(pc)–1 was prepared by direct cyclization in a melt[32] of phthalonitrile and hydroquinone in a sealed, partially evacuated quartz tube. A typical preparation employed 4 g (30 mmol) of phthalonitrile and 1 g (9 mmol) of hydroquinone. Quartz and Teflon vessels were necessary to avoid contamination of the macrocycle by metal ions. The crude product was washed thoroughly with hot water and acetone and subsequently sublimed twice at 400 °C (less than 10^{-3} Torr). The yield of H_2(pc)–1 was 53% after sublimation. H_2(pc)–2 was prepared by subliming twice at 450 °C (less than 10^{-3} Torr) H_2(pc) recently obtained from Kodak. H_2(pc)–3 designates H_2(pc) purchased from Kodak and purified by sublimation by previous workers in this laboratory. However, none of this parent material remained for the present study.

Synthesis of Ni(pc). This compound was prepared by four methods. Within error, each preparation gave the same satisfactory elemental analysis.

Method 1. A 1.00-g (1.94-mmol) sample of H_2(pc)–1 was metalated with 0.92 g (3.88 mmol) of 99.9985% $NiCl_2 \cdot 6H_2O$ (Johnson Matthey) in 20 mL of a 10% quinoline/1-chloronaphthalene solvent system. The solution was refluxed in a quartz vessel for 72 h and then cooled in an ice bath. The purple Ni(pc)–1 crystals that precipitated were removed by filtration and washed with hot water and acetone. The progress of the metalation was followed by UV–vis spectroscopy, and the reaction was repeated until the peak at 696 nm in the UV–vis spectrum associated with H_2(pc) was removed. The resulting material was sublimed twice in vacuum at 400 °C. The yield of Ni(pc)–1 was 0.62 g (56% based on H_2(pc)).

Method 2. A 2.00-g (15.6-mmol) sample of phthalonitrile was cyclized with 0.76 g (4.3 mmol) of 99.999% anhydrous $Ni(OCOCH_3)_2$ (Johnson Matthey) and 0.48 g (4.4 mmol) of hydroquinone in 6 mL of quinoline. The solution was refluxed under nitrogen for 5 h and then cooled. The resulting precipitate was collected and washed with hot water and acetone. Purification by sublimation gave 0.47 g (21% yield) of Ni(pc)–2.

Method 3. A 2.0-g (15.6-mmol) sample of phthalonitrile was cyclized with 1.0 g (7.8 mmol) of 99.9985% anhydrous $NiCl_2$ (Johnson Matthey) in 4 mL of quinoline. The solution was refluxed for 10 min until the solution solidified. The solid mixture was ground, washed with acetone and hot water, and sublimed twice to afford 1.02 g (46% yield) of Ni(pc)–3.

Method 4. A 2.0-g (15.6-mmol) sample of phthalonitrile was cyclized with 1.43 g (8.6 mmol) of 99.999% anhydrous $Ni(OCOCH_3)_2$ (Johnson Matthey) in 4 mL of quinoline under nitrogen. The solution was refluxed for 3 h and then cooled. The precipitate was washed with acetone and methanol, and sublimed twice to afford 0.50 g (23% yield) of Ni(pc)–4.

Iodine Oxidation. Each oxidized material is numbered according to the parent material used in its preparation. Single crystals of H_2(pc)I–*i*, $i = 1$ and 2, were grown by oxidation of the parent material in 1-chloronaphthalene at 110 °C, in quartz H-tubes, in the presence of a large excess of I_2. Shiny dark-green crystals of H_2(pc)I–*i*, $i = 1$ and 2, were collected by filtration. H_2(pc)–3 was oxidized by I_2 in 1,2,4-trichlorobenzene at 95 °C in Pyrex H-tubes to give H_2(pc)I–3. Single crystals of all Ni(pc)I–*j* compounds, $j = 1$–4, were prepared by the same method used for H_2(pc)I–1,2 except the crystals were grown at 170 °C.

X-ray Diffraction Study of H_2(pc)I. Single crystals of H_2(pc)I–1 used for the data collection were grown as described above. The final cell dimensions of $a = 13.931(2)$ Å and $c = 6.411(1)$ Å at 108 K were found by a least-squares refinement of the setting angles of 24 reflections that had been automatically centered on an Enraf-Nonius CAD4 diffractometer.

Intensity data were collected at 108 K by the ω–2θ scan technique and were processed by methods standard to this laboratory.[33] No systematic changes were observed in the intensities of the six standard reflections that were measured every 3 h of X-ray exposure time. A total of 748 unique reflections were measured, 702 of which were found to have $F_o > 3\sigma(F_o)$. An absorption correction was applied.[34] Experimental details and crystal data are shown in Table I. Further details are given in Table IS.

The systematic absences are consistent with space group D_{4h}^2 – $P4/mcc$. As Ni(pc)I, Cu(pc)I, Co(pc)I, Fe(pc)I, Ni(tbp)I (tbp = tetrabenzoporphyrinato), and H_2(tbp)I all belong to this space group,[17,20-22,35,36] we assumed that H_2(pc)I also does. Successful refinement of the structure supports this choice. The positions of the carbon and nitrogen atoms were assumed initially to be those for Ni(pc)I. After subsequent refinement of the structure,[37] the positions of the hydrogen atoms were calculated. By symmetry the two hydrogen atoms bound to the pyrrole nitrogen atoms are disordered over the four sites. The final refinement on F_o^2, including anisotropic thermal parameters for all non-hydrogen atoms and a riding model for the hydrogen atoms (64 variables, 702 observations) resulted in a value for R_w of 0.059. For those reflections having $F_o^2 > 2\sigma(F_o^2)$, $R(F)$ is 0.030. A final difference electron density map showed no unusual features. Final positional and thermal parameters are given in Table II. Table IIS presents anisotropic displacement coefficients.

Resonance Raman Spectroscopy. Raman spectra of H_2(pc)I–1 were obtained as described earlier.[20,38]

Table I. Crystallographic Data for H_2(pc)I

formula	$C_{32}H_{18}IN_8$	density (calcd), g/cm^3	1.712
fw, amu	641.4	radiation ($\lambda(K\alpha_1)$, Å)	graphite-monochromator (0.7093)
space group	$D_{4h}^2 - P4/mcc$		
a, Å	13.931(2)	μ, cm^{-1}	13.1
c, Å	6.411(1)	transm factors	0.921–0.939
V, Å^3	1244.2(6)	$R(F)$ ($F_o^2 > 2\sigma(F_o^2)$)	0.030
Z	2	$R_w(F^2)$	0.059
temp, K	108	goodness of fit	1.58

(29) Ferraro, J. R.; Williams, J. M. *Introduction to Synthetic Electrical Conductors*; Academic Press: Orlando, FL, 1987; pp 263–285.
(30) Cowan, D. O.; Wiygul, F. M. *Chem. Eng. News* **1986**, *64*(29), 28–45.
(31) Jerome, D.; Creuzet, F.; Bourbonnais, C. *Phys. Scr.* **1989**, *T27*, 130–135.
(32) Snow, A. W.; Jarvis, N. L. *J. Am. Chem. Soc.* **1984**, *106*, 4706–4711.
(33) Corfield, P. W. R.; Doedens, R. J.; Ibers, J. A. *Inorg. Chem.* **1967**, *6*, 197–204.
(34) de Meulenaer, J.; Tompa, H. *Acta Crystallogr.* **1965**, *19*, 1014–1018.
(35) Martinsen, J.; Pace, L. J.; Phillips, T. E.; Hoffman, B. M.; Ibers, J. A. *J. Am. Chem. Soc.* **1982**, *104*, 83–91.
(36) Murata, K.; Thompson, J. A.; McGhee, E. M.; Hoffman, B. M.; Ibers, J. A. Manuscript in preparation.
(37) Sheldrick, G. M. SHELXL-92, Unix Beta-Test Version.
(38) Shriver, D. F.; Dunn, J. B. R. *Appl. Spectrosc.* **1974**, *28*, 319–323.

Table II. Atomic Coordinates and Equivalent Isotropic Displacement Coefficients (Å²)

atom	x	y	z	U_{eq}
I	1/2	1/2	1/4	0.0348(2)
N(1)	0.1276(2)	0.0602(2)	0	0.0136(14)
N(2)	0.0821(2)	0.2282(2)	0	0.015(2)
C(1)	0.1453(3)	0.1571(3)	0	0.014(2)
C(2)	0.2490(2)	0.1727(2)	0	0.014(2)
C(3)	0.3042(2)	0.2556(3)	0	0.018(2)
C(4)	0.4032(3)	0.2446(2)	0	0.021(2)
C(5)	0.4458(2)	0.1535(3)	0	0.021(2)
C(6)	0.3903(2)	0.0706(3)	0	0.018(2)
C(7)	0.2917(2)	0.0819(2)	0	0.014(2)
C(8)	0.2133(2)	0.0120(3)	0	0.0147(13)
H(1)	0.0691	0.0327	0	0.018
H(2)	0.2757	0.3167	0	0.023
H(3)	0.4425	0.2995	0	0.028
H(4)	0.5131	0.1483	0	0.027
H(5)	0.4186	0.0094	0	0.023

Single-Crystal Electrical Conductivity Studies. Single crystals of both H_2(pc)I–*i* and Ni(pc)I–*j* were mounted on graphite fibers with a locally prepared palladium paste. Four-probe constant current ac (27 Hz) conductivity measurements were performed along the stacking axis. All crystals showed ohmic properties at all temperatures studied over the current range 10^{-6}–10^{-3} A. As a result of the high conductivity first observed for H_2(pc)I–1, the apparatus previously described had to be modified.[39] A Stanford Research SR-530 two-channel lock-in amplifier in differential mode was used to measure the voltage drop along the sample. The two voltage leads from the crystal sample holder to the lock-in amplifier and the two current leads were heavily shielded and grounded to the brass sample holder. Some conductivity measurements were performed between 300 and 6 K in cold He gas as described; the temperature was monitored with a silicon diode sensor (Lakeshore Cryotronics, Model DT 470) located in the vicinity of the sample. Conductivity measurements from 300 to 1.9 K and magnetoconductivity employed a Quantum Design SQUID susceptometer to apply a transverse field up to 5 T and to control the temperature. The dimensions of the sample chamber made it very difficult to measure the longitudinal magnetoconductivity. The conductivity measurements were made on several crystals from each batch of oxidized material and the relative conductivity, $\sigma_{rel} = \sigma(T)/\sigma(300\ K)$, was highly reproducible between crystals of a given batch. Absolute conductivities vary between crystals, presumably as a consequence of uncertainties in measurements of the crystal dimensions.

Measurements of Magnetic Properties. EPR measurements were performed as described.[20,21] The level of Cu(pc) impurities present in the parent M(pc) materials was determined by comparing the signal intensity at 77 K to that of $Cu_{0.01}H_{2(0.99)}$(pc).

Static magnetic susceptibility measurements were taken from 300 to 1.9 K with a Quantum Design SQUID susceptometer. Gelatin capsules were used to hold the samples and the background was measured over the full temperature range just prior to measuring the sample. Data were recorded at 5 kG on samples of 20–40 mg. The core susceptibilities also were measured. They are -3.73×10^{-4} emu/mol for H_2(pc)I–1, -4.16×10^{-4} emu/mol for Ni(pc)–1, and -4.30×10^{-4} emu/mol for Ni(pc)–3.

Results and Discussion

Purity of the M(pc) Parent Macrocycles. Neither H_2(pc) nor Ni(pc) should exhibit an EPR signal as H_2(pc) is a closed-shell aromatic molecule and Ni^{II} is diamagnetic in square-planar coordination. Nonetheless, EPR signals at $g = 2$ are invariably observed for these two compounds (Figures 1 and 2).[40,41] In addition, H_2(pc) shows signals from paramagnetic Cu(pc), which is present as an impurity,[8,9,42] and we have detected Co(pc) as well. Thus, the EPR spectra of M(pc) serve as measures of their purity.

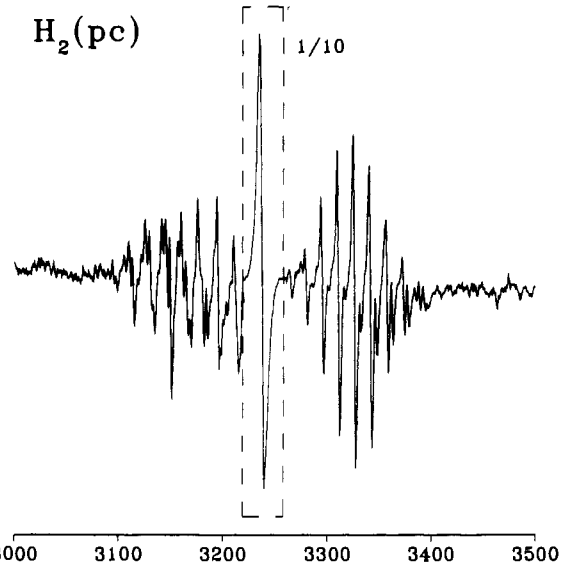

Figure 1. X-Band EPR spectrum of H_2(pc)–2 at 77 K showing a free-radical signal centered at $g = 2$ and Cu–N hyperfine structure from Cu(pc) impurities. The radical signal has been reduced 10-fold.

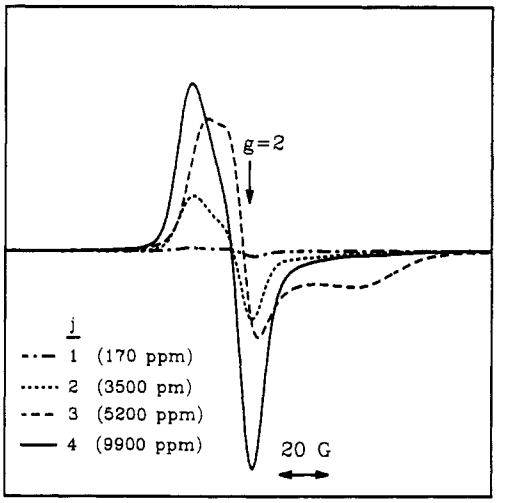

Figure 2. EPR spectra of Ni(pc)I–*j*, *j* = 1–4, powders taken at room temperature.

As an example, the EPR spectrum of a sample of commercially obtained H_2(pc)–2 is dominated by a strong Lorentzian-shaped EPR signal centered at $g = 2$ with a peak-to-peak linewidth of 6 G (Figure 1). Double integration of the free-radical signal and comparison with the DPPH reference indicate that the material contains ca. 300 ppm $S = 1/2$, $g = 2$ spins. However, this value varies among different batches of H_2(pc) purchased from Kodak. The spectrum also shows the distinctive multiline signal arising from the presence of Cu(pc) as an impurity. Comparison of the EPR signal from Cu(pc) with a $Cu_{0.01}H_{2(0.99)}$(pc) standard prepared for this purpose reveals that there are ca. 1300 ppm Cu(pc) present in H_2(pc)–2. To eliminate the Cu(pc) impurities, we prepared our own H_2(pc) from purified hydroquinone and phthalonitrile. However, these materials also show EPR signals from Cu(pc), with the Cu presumably scavenged from the Pyrex reaction vessel. If the reaction is done in rigorously cleaned quartz or Teflon containers, the Cu(pc) impurity is <100 ppm for H_2(pc)–1; only an upper limit may be assigned because the EPR signal is so weak. Data for the *g* value of H_2(pc)I–1 presented below also require a concentration of <100 ppm. This preparation procedure also reduces the free-radical impurity from ca. 300 ppm in H_2(pc)–2 to ca. 60 ppm in H_2(pc)–1. This suggests that the organic ($g = 2$) radicals are formed in a reaction catalyzed by metal ions. Although both the organic radical and Cu(pc)

(39) Phillips, T. E.; Anderson, J. R.; Schramm, C. J.; Hoffman, B. M. *Rev. Sci. Instrum.* **1979**, *50*, 263–265.
(40) Assour, J. M.; Harrison, S. E. *J. Phys. Chem.* **1964**, *68*, 872–876.
(41) Raynor, J. B.; Robson, M.; Torrens-Burton, A. S. M. *J. Chem. Soc., Dalton Trans.* **1977**, 2360–2364.
(42) Harbour, J. R.; Loutfy, R. O. *J. Phys. Chem. Solids* **1982**, *43*, 513–520.

Table III. Impurity Levels and Conductivity Characteristics of H_2(pc)I and Ni(pc)I Compounds[a]

compd	σ_{rel}^{max}	T_{max}, K	radical impurities, ppm
H_2(pc)I–1	31	3	60
H_2(pc)I–2	17 (6 K)[b]		300
H_2(pc)I–3	8	15	*c*
H_2(pc)I[d]	6–7	15	*c*
H_2(pc)I[e]	5	25	*c*
Ni(pc)I–1	29	5	170–250
Ni(pc)I–2	6	15	3400
Ni(pc)I–3	3	40	5200
Ni(pc)I–4	2	60	9900
Ni(pc)I[f]	5.5	25	*c*
Ni(pc)I[g]	~2	~70	*c*

[a] H_2(pc)I–*i* and Ni(pc)I–*j* were prepared from the corresponding parent macrocycle, and the synthesis of these is described in the Experimental Section. [b] Value of relative conductivity at 6 K, the lowest temperature measured. [c] Not available for study. [d] References 18 and 19; commercial H_2(pc). [e] Reference 28; commercial H_2(pc). [f] Reference 16; commercial Ni(pc). [g] References 13 and 14; commercial Ni(pc).

impurities have been reduced, the shape of the EPR signal of H_2(pc)–1 is similar to that of H_2(pc)–2 with a peak-to-peak line width of 4 G at room temperature.

The preparation of pure Ni(pc) is more difficult. In the course of parallel studies on Zn(tbp), we found that Cu^{II}, Co^{II}, and Fe^{II} could be incorporated from impurities in reagent grade Zn salts. Thus, we prepared Ni(pc)–*j*, *j* = 2–4, from high-purity Ni salts via the template reaction with phthalonitrile described above; these products show no detectable EPR signals from Cu(pc), but they do show strong $g = 2$ signals (Figure 2). Double integration of the EPR spectra of Ni(pc)–*j*, *j* = 2–4, gives 3400–9900 ppm $S = {}^1/_2$ spins, Table III. The different preparation methods produce compounds whose EPR signals have different shapes; this suggests that more than one type of radical contributes to the signals. In an attempt to reduce the level of organic impurities, we prepared Ni(pc)–1 by metalation of pure H_2(pc)–1 with Ni^{II} salts, and this led to the purest Ni(pc) material studied, with only 170–250 ppm organic radical impurities and no detectable Cu(pc) signal. The decreased level of organic impurities in a preparation that did not employ a template synthesis of the pc ring supports the idea that these impurities are products of a metal-catalyzed reaction.

A surprising result of this work is that the impurities responsible for the $g = 2$ signal cannot be removed by the final purification step of vacuum ($P < 10^{-3}$ Torr) sublimation at $T > 400$ °C. Such signals have been assigned in many ways: for example, as complexes between M(pc) and oxygen[40] or as trapped charge carriers at structural defects or impurity sites.[42] The fact that the signal persists after multiple sublimations *in vacuo* leads us to assign them to suprisingly stable, free-radical organic impurities in both Ni(pc) and H_2(pc). The availability of a series of Ni(pc)–*j*, *j* = 1–4, materials with a wide range of impurity levels enabled us to study the effects of impurities on various physical properties, primarily the single crystal conductivity of Ni(pc)I.

Structure of H_2(pc)I. Structurally, H_2(pc)I–1 is nearly identical to its Ni analogue.[17] The macrocycles are stacked in chains that run parallel to the *c* axis, with chains of iodine atoms in the channels between the stacks. This arrangement can be seen in the drawing of the unit cell of H_2(pc)I (Figure 3). The two H_2(pc) molecules within the unit cell are staggered by 40°. The phthalocyanine macrocycle is necessarily planar because all atoms in the molecule lie upon a site of 4/*m* symmetry. The two central H atoms are disordered over the four central sites. Figure 4 shows a perspective view of the H_2(pc) molecule with labeling scheme. The thermal parameter of the iodine atom along the *c* axis, U_{33}, is four times larger than those along the *a* axes, U_{11} and U_{22} (Table IIS). This has been observed for Ni(pc)I where diffuse scattering measurements were interpreted in terms of ordered chains of linear triiodide anions, disordered with respect to their

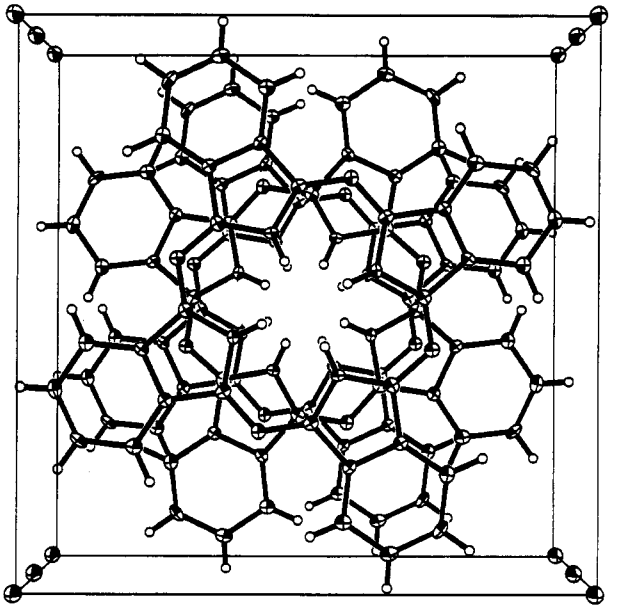

Figure 3. Unit cell of H_2(pc)I–1 viewed down the *c* axis.

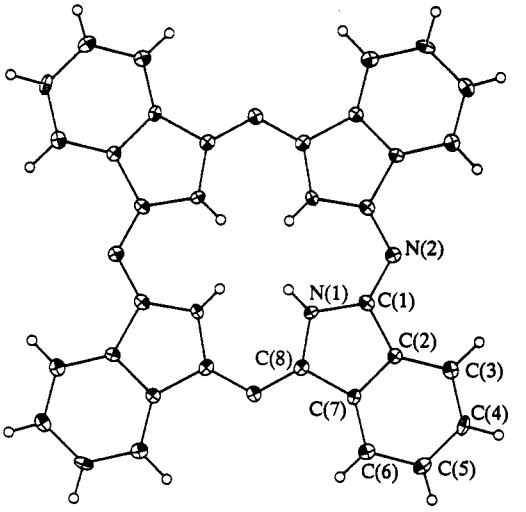

Figure 4. Drawing of the H_2(pc)I–1 molecule with labeling scheme. Thermal ellipsoids are drawn at 50% probability level.

origins. Moreover, the resonance Raman spectrum of crystalline H_2(pc)I–1 shows a sharp peak at 107 cm^{-1} with an overtone progression of peaks at 215, 320, and 428 cm^{-1}. This pattern is typical for linear chains of symmetrical triiodide ions.[43,44] We thus conclude that the model for the anion deduced for Ni(pc)I holds for H_2(pc)I–1 as well.

Bond distances and angles are given in Table IV. Replacement of a central metal atom with protons enlarges the central hole. Thus, the distance from the center of the macrocycle to the nitrogen atoms is 1.969(4) Å, compared to 1.887(6) Å in Ni(pc)I;[17] the angle at the nitrogen atom is also larger, 109.3(3) vs 106.3(3)°.[17]

Physical Properties of M(pc)I, M = H_2 and Ni. Charge Transport. Figure 5 shows the temperature-dependent conductivities of H_2(pc)I–1 and Ni(pc)I–1 normalized to their room-temperature values. The average room-temperature conductivity of each material is ~500 Ω^{-1} cm^{-1}. This value is similar to published results on these two compounds[16-19] and to those seen for the other materials studied here. As the temperature is lowered, the conductivities of both H_2(pc)I–1 and Ni(pc)I–1

(43) Teitelbaum, R. C.; Ruby, S. L.; Marks, T. J. *J. Am. Chem. Soc.* **1978**, *100*, 3215–3217.
(44) Teitelbaum, R. C.; Ruby, S. L.; Marks, T. J. *J. Am. Chem. Soc.* **1980**, *102*, 3322–3328.

Table IV. Bond Distances (Å) and Angles (deg) for $H_2(pc)I$

bond	distance	bond	angle
N(1)–C(1)	1.372(4)	C(8)–N(1)–C(1)	109.0(3)
N(1)–C(8)	1.370(4)		
		C(1)–N(2)–C(8)	122.6(3)
N(2)–C(1)	1.325(5)		
N(2)–C(8′)	1.328(5)	N(2)–C(1)–N(1)	128.1(3)
		N(2)–C(8)–N(1)	128.3(3)
C(1)–C(2)	1.461(5)		
C(7)–C(8)	1.462(4)	N(1)–C(1)–C(2)	108.9(3)
		N(1)–C(8)–C(7)	108.9(3)
C(2)–C(3)	1.388(5)		
C(6)–C(7)	1.383(5)	N(2)–C(1)–C(2)	123.0(3)
		N(2)–C(8)–C(7)	122.7(3)
C(3)–C(4)	1.388(5)		
C(5)–C(6)	1.390(5)	C(3)–C(2)–C(1)	132.2(3)
		C(6)–C(7)–C(8)	131.7(3)
C(2)–C(7)	1.397(4)		
		C(7)–C(2)–C(1)	106.6(3)
C(4)–C(5)	1.402(5)	C(2)–C(7)–C(8)	106.5(3)
		C(3)–C(2)–C(7)	121.1(3)
		C(6)–C(7)–C(2)	121.7(3)
		C(4)–C(3)–C(2)	117.4(3)
		C(7)–C(6)–C(5)	117.3(3)
		C(3)–C(4)–C(5)	121.3(3)
		C(6)–C(5)–C(4)	121.1(3)

increase dramatically until they reach, respectively, maxima at $T_{max} \sim 3$ or 5 K with $\sigma_{rel}^{max} = \sigma(T_{max})/\sigma(300\ K) \approx 31$ or 29 that correspond to absolute conductivities of (1–2) × 10^4 Ω^{-1} cm^{-1} (Figure 5). With further cooling of the sample the conductivity of each decreases slightly: at 1.85 K the conductivity of H_2-(pc)I–1 has dropped by only 7% from its maximum, and that of Ni(pc)I–1 by 38%. Preliminary experiments with $H_2(pc)I$–1 carried out down to 20 mK show that the conductivity does not tend toward zero as $T \rightarrow 0$ K, but reaches a plateau with $\sigma_{rel} \approx 18$.[45] The fall-off in conductivity for $T < T_{max}$ appears to be more substantial for Ni(pc)I–1 than for $H_2(pc)I$–1 (see inset in Figure 5) because T_{max} is a few degrees higher. Very low temperature studies will be done on Ni(pc)I–1 to see if it behaves similarly.

$H_2(pc)I$–1 and Ni(pc)I–1 are the first examples of macrocyclic molecular conductors exhibiting metallic temperature dependence over such a wide temperature range, and their absolute conductivities of (1–2) × 10^4 Ω^{-1} cm^{-1} at 3–5 K are unprecedented. These data may be contrasted with results for $H_2(pc)I$–3 and Ni(pc)I–3, which are representative of the temperature dependence of material prepared from purified commercial $H_2(pc)$ and Ni(pc) and are similar to published data;[13,14,16,18,19,28,46] see Table III. At temperatures below $T \sim 200$ K, the conductivities of $H_2(pc)I$–3 and Ni(pc)I–3 are markedly reduced compared to $H_2(pc)I$–1 and Ni(pc)I–1; their maximum conductivities of $\sigma_{rel}^{max} \approx 3$–8 are much lower and occur at much higher temperatures (Figure 5 and Table III). For Ni(pc)I–3, at temperatures below T_{max} the conductivity tends to zero as T decreases, just as theory predicts for localization of the electrons by impurities in one-dimensional systems.[47] More data would be required to clarify the very low T behavior of $H_2(pc)I$–3.

Intermediate behavior is shown by $H_2(pc)I$–2, which was prepared from a different batch of commercial $H_2(pc)$. Its conductivity is much greater than that of $H_2(pc)I$–3, with σ_{rel}(6 K) = 17 and with $T_{max} < 6$ K, the lowest temperature measured. However, the conductivity at 6 K is much lower than that for the purest material, $H_2(pc)I$–1 (Table III). This result highlights the variability of the conductivity of $H_2(pc)I$ prepared from commercial parent material.

(45) Hensley, H.; Lee, Y.; Halperin, W. P.; Thompson, J. A.; Hoffman, B. M. Manuscript in preparation.
(46) Martinsen, J.; Greene, R. L.; Palmer, S. M.; Hoffman, B. M. *J. Am. Chem. Soc.* **1983**, *105*, 677–678.
(47) Nagaoka, Y. *Prog. Theor. Phys. Suppl.* **1985**, No. 84, 1–15.

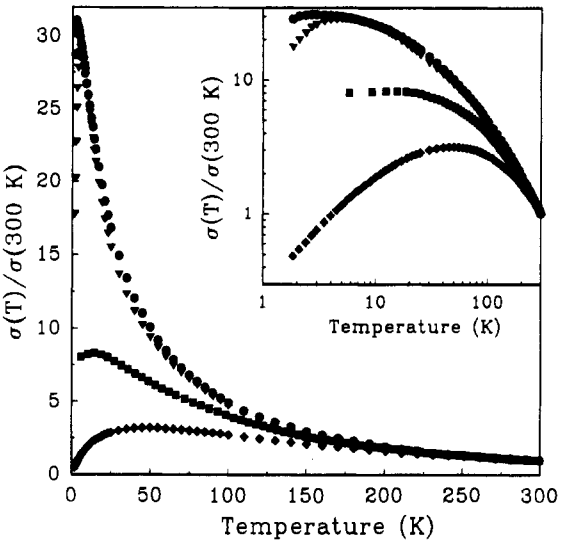

Figure 5. Normalized single-crystal conductivity for $H_2(pc)I$–1 (●), $H_2(pc)I$–3 (■), Ni(pc)I–1 (▼) and Ni(pc)I–3 (◆). Inset: Log–log plot of normalized conductivity.

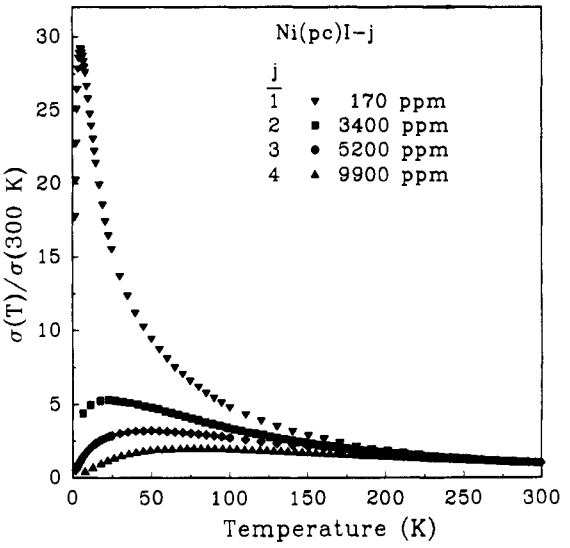

Figure 6. Temperature-dependent conductivities of Ni(pc)I–j, j = 1–4.

Correlations of Conductivity and Purity. The possibility that impurities from the parent macrocycle may have controlled the low-temperature conductivity in previous studies of the M(pc)I and related materials has been addressed with studies of a set of Ni(pc)I compounds. The normalized conductivities for Ni(pc)I–j, j = 1–4 are shown in Figure 6. The room-temperature conductivities are all the same within experimental error, but at low temperatures there are dramatic variations in σ that may be correlated to the level of $g - 2$ impurities in the parent macrocycle. As described above, the conductivity of Ni(pc)I–1 shows a metallic increase as the temperature decreases, reaching $\sigma_{rel}^{max}(T) = 29$ at 5 K. As the level of free-radical impurities in the parent material increases for Ni(pc)I–j, j = 2–4, the conductivity of the conductors, as exemplified by the maximum conductivity (σ_{rel}^{max}), decreases and T_{max} shifts to higher temperatures (Table III) signifying that the onset of localization of the charge carriers occurs at progressively higher temperatures. In previously published results on Ni(pc)I prepared from multiply sublimed commercial material, σ_{rel}^{max} varies from 2 to 6 and T_{max} varies from 25 to 70 K (Table III).[13,14,16,46] From Figure 7, which shows the correlation between the level of free-radical impurities in the parent material and the maximum conductivity, one may infer that a $\sigma_{rel}^{max} \approx 6$ corre-

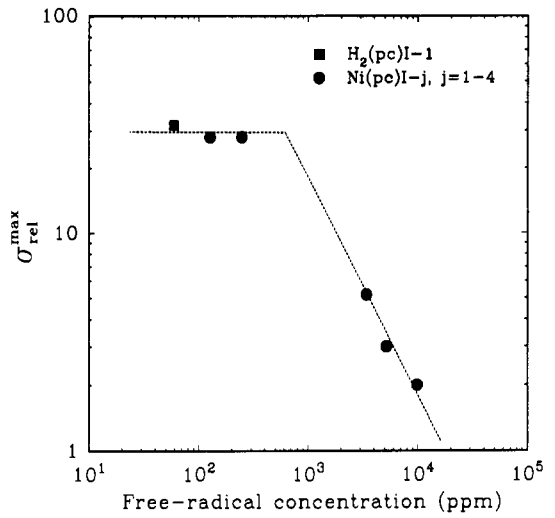

Figure 7. Plot of σ_{rel}^{max} for the various M(pc)I, M = "H_2", Ni, versus the free-radical impurity concentration in the parent M(pc) material utilized in the preparation. The dashed line is included to guide the eye.

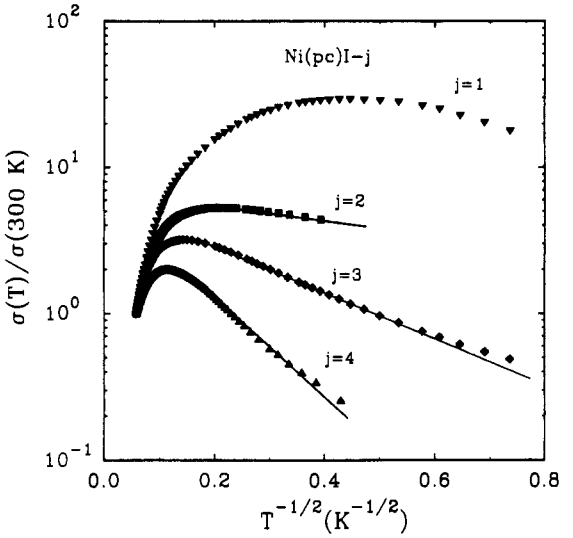

Figure 8. Plot of normalized conductivity vs $T^{-1/2}$ for Ni(pc)I-j, j = 1–4. For j = 2–4, the normalized conductivity shows a linear dependence on $T^{-1/2}$ as expected for phonon-assisted hopping as described in the text.

sponds to an impurity level ca. 60 times greater than that in H_2(pc)I-1, with $\sigma_{rel}^{max} \approx 31$.

The occurrence of a conductivity maximum that varies with purity level may be understood in terms of an interplay between phonon scattering and localization of one-dimensional carrier electrons by impurities. As the temperature is lowered, phonon scattering decreases and the conductivity tends to increase, whereas electron localization by defects or impurities increases and lowers the conductivity. The result is a conductivity maximum. As the impurity concentration becomes greater, electron localization becomes more dominant, and the conductivity maximum decreases and moves to higher temperatures. Electron localization can be described by a model that involves variable-range hopping; the following temperature-dependence is predicted[48,49]

$$\sigma_{rel} \propto \exp(-T_0/T)^{1/2} \qquad (1)$$

Figure 8 shows plots of log σ versus $T^{-1/2}$ for Ni(pc)I-j, j = 1–4. At temperatures below T_{max}, the materials Ni(pc)I-j, j = 2–4 but *not* j = 1, show the linear dependence of log σ on $T^{-1/2}$ expected from eq 1. This result suggests that the conductivity of Ni(pc)I-j, j = 2–4, at low temperatures is limited by one-dimensional variable-range hopping resulting from the random potential created by impurities or crystal defects. It further suggests the possibility that the temperature dependence of the conductivity of Ni(pc)I-1 and by inference the conductivity of H_2(pc)I-1 represent the intrinsic properties of these materials. We return to this below.

Although the repression of the conductivity owing to increased impurity concentration is most obvious at temperatures near or below T_{max}, effects also can be seen at higher temperatures. In general, as a metal is cooled from room temperature there is a broad temperature range over which the relative resistivity, $\rho_{rel}(T) = \rho(T)/\rho(295\ K)$, can be described by the expression[50]

$$\rho_{rel}(T) = a + b(T/295\ K)^{\gamma} \qquad (2)$$

This equation, though not a completely adequate description of the charge transport properties, is useful for examining the trends in the parameters that describe a series of materials. All these materials show a temperature range where eq 2 applies, with $\gamma \sim 1.65$–1.85, consistent with results for most molecular metals and in contrast to those for conventional metals, where $\gamma \approx 1$.[51] The difference among the H_2(pc)I-i, i = 1–3, and Ni(pc)I-j, j = 1–4, materials is the temperature range over which each remains metallic and eq 2 is obeyed: the purer the compound, the lower the temperature to which eq 2 holds. There also are some general trends for the coefficients in eq 2. The term a would represent the residual resistivity if eq 2 had been applicable down to low temperatures, and thus it might be expected to be proportional to the defect concentration. In fact, a weakly increases in a linear fashion with the concentration of paramagnetic defects in the parent M(pc) materials from $a \approx 0.05$ in the purest material ($[R^{\bullet}]$ = 60 ppm) to $a \approx 0.4$ when $[R^{\bullet}] \approx 10^4$ ppm. The terms b and γ are not expected to vary with the defect concentration because they represent intrinsic charge transport properties. Nonetheless, b decreases (8.9×10^{-5} to 1.5×10^{-5}) and γ increases slightly (1.65 to 1.85) with increasing defect concentration. Similar trends in a were seen in a study of the effects of radiation-induced defects on the charge-transport properties of tetrathiafulvalene–tetracyanoquinodimethane (TTF-TCNQ).[52] However, γ was found to be invariant to the defect concentration and the term proportional to b actually increased with increasing defect concentration.[52]

Magnetoconductivity. We have measured the magnetoconductivity of H_2(pc)I-1 and Ni(pc)I-1 to explore further the nature of the conductivity maximum in these pure materials. For temperatures down to 40 K, the magnetoconductivity, represented as the fractional change in the conductivity upon application of a 5 T transverse magnetic field, $\Delta\sigma/\sigma$, is approximately zero for both compounds. As the temperature decreases further, application of an external magnetic field decreases the conductivity slightly, with $\Delta\sigma/\sigma$ reaching its largest value of –4% at $T_{max} \approx$ 3 K for H_2(pc)I-1 and –3.5% at $T_{max} \approx 5$ K for Ni(pc)I-1. Such small negative values are rather typical for conventional metals, where the conductivity decreases slightly upon application of a magnetic field because of magnetic forces on the moving charges.[53] This suggests that these M(pc)I materials are acting like "normal" metals and that the conductivity maximum is not associated with scattering of the conduction electrons by local moments of paramagnetic metals. In the latter case the conductivity would

(48) Bloch, A. N.; Weisman, R. B.; Varma, C. M. *Phys. Rev. Lett.* **1972**, *28*, 753–756.
(49) Mott, N. F. *Philos. Mag.* **1969**, *19*, 835–852.
(50) Seiden, P. E.; Cabib, D. *Phys. Rev. B: Solid State* **1976**, *13*, 1846–1849.
(51) Williams, J. M.; Ferraro, J. R.; Thorn, R. J.; Carlson, K. D.; Geiser, U.; Wang, H. H.; Kini, A. M.; Whangbo, M.-H. *Organic Superconductors (Including Fullerenes): Synthesis, Structure, Properties, and Theory*; Prentice-Hall: Englewood Cliffs, NJ, 1992; pp 118–123.
(52) Chiang, C. K.; Cohen, M. J.; Newman, P. R.; Heeger, A. J. *Phys. Rev. B: Solid State* **1977**, *16*, 5163–5172.
(53) Kittel, C. *Quantum Theory of Solids*, 2nd ed.; John Wiley & Sons: New York, 1987; Chapter 12; pp 237–248.

increase upon application of the magnetic field as seen in Cu_xNi_{1-x}(pc)I alloys.[54]

EPR Spectroscopy and Magnetic Susceptibility. Powder samples of H_2(pc)I–1 and Ni(pc)I–1 exhibit an axial EPR signal centered around $g = 2$ with a Lorentzian line shape and $g_\parallel$ aligned along the c axis. Within experimental error, the g values for both materials are temperature-independent from 300 to 1.9 K: $g_\parallel$(Ni) = 2.008(1), $g_\parallel(H_2)$ = 2.006(1); $g_\perp$(Ni) = $g_\perp(H_2)$ = 2.001(1). This result can be used independently to set an upper bound to the concentration of Cu(pc) impurities within these molecular metals. We showed earlier that exchange coupling between local Cu^{II}, $S = {}^1/_2$, metal ions and itinerant spins in Cu_xNi_{1-x}(pc)I results in temperature-dependent g values, with shifts in the g values that are proportional to the Cu concentration and inversely proportional to temperature.[20,55] If the lack of any observed change in $g_\parallel$ as T is lowered from 300 to 1.9 K is taken to mean that $g_\parallel$ increases by less than ca. twice the experimental uncertainty, $\delta g_\parallel \approx 2 \times 10^{-3}$, then according to eq 3 in ref 55 the concentration of paramagnetic Cu^{II} in H_2(pc)I–1 and Ni(pc)I–1 must be less than ~25 ppm, consistent with the quantitative analysis of the EPR spectrum of the parent macrocycles, H_2(pc)–1 and Ni(pc)–1 (*vide supra*).

Fits of the EPR powder patterns of Ni(pc)I–1 and H_2(pc)I–1 show that both have small line widths of $\Gamma_\parallel \approx 8$–10 MHz and $\Gamma_\perp \approx 6$–7 MHz at room temperature; those for Ni(pc)I–1 do not change upon cooling the sample to 2 K, whereas those of H_2(pc)I–1 increase to $\Gamma_\parallel \approx 20$ and $\Gamma_\perp \approx 11$ MHz. Although both H_2(pc)I–1 and Ni(pc)I–1 exhibit a conductivity maximum at ~3–5 K (*vide supra*), there are no changes in the EPR spectra between 4.2 and 2 K. Metal-to-nonmetal phase transitions typically are accompanied by a change in the EPR line width below the conductivity maximum.[56] The absence of such an effect suggests that there is no such phase transition at T_{max} for either H_2(pc)I–1 or Ni(pc)I–1.

The previous data on the room-temperature line widths of Ni(pc)I prepared from commerical material gave a similar value for $\Gamma_\perp$ for Ni(pc)I–1, but $\Gamma_\parallel$ was significantly larger and both $\Gamma_\parallel$ and $\Gamma_\perp$ decreased with decreasing temperature.[16,17] To clarify this difference from Ni(pc)I–1, we collected EPR spectra for Ni(pc)I–3, which has charge-transport properties similar to those of Ni(pc)I prepared from commercial material. Although the room-temperature line widths for Ni(pc)I–3 are similar to those of both H_2(pc)I–1 and Ni(pc)I–1, these widths decrease ca. 3-fold with decreasing temperature. This is consistent with the original reports for Ni(pc)I prepared from commercial Ni(pc)[16,17] and indicates that this behavior may be attributed to the presence of impurities at levels greater than that in Ni(pc)I–1. The decrease in line width at low temperatures in the more poorly conducting materials may be associated with a decrease in the density of states at the Fermi level resulting from localization of the conduction electrons.[57]

We also investigated[58] the static susceptibility χ for H_2(pc)I–1, Ni(pc)I–1, and Ni(pc)I–3. In each case, χ is virtually temperature-independent from 300 to 30 K, as expected for a metallic conductor with temperature-independent Pauli paramagnetism. Below 30 K, χ shows a modest increase for each of the three substances. The absence of any parallel increase in χ in single-crystal EPR measurements[17] supports an assignment to physical defects in the powder sample used for the susceptibility measurements. The absence of unusual features or changes in the susceptibility around $T \approx T_{max}$ is further evidence that the conductivity maxima are not due to phase transitions.[59]

The Pauli paramagnetism, χ_P, for H_2(pc)I–1, Ni(pc)I–1, and Ni(pc)I–3 was determined (i) by double integration of the room-temperature EPR signal with DPPH as a standard and (ii) from the room-temperature static susceptibility, as well as (iii) from a fit of the variable-temperature susceptibility data to a Curie–Weiss law plus a term for the temperature-independent Pauli paramagnetism, $\chi(T) = \chi_P + C/(T - \theta)$. We calculated the transfer integral (t) that represents the intrachain, intermolecular coupling of the p–π molecular orbitals comprising the one-dimensional tight-binding conduction band for each material from the average of χ_P from the three techniques.[60] The values fell in the range $4t \approx 0.28$–0.41 eV. These values are in good agreement with published results, but are smaller than those obtained from optical or thermopower measurements, $4t \approx 0.8$–1.3 eV.[14,16,18] The discrepancy is attributable to Coulomb effects, which lower $4t$ as calculated from χ_P.[61,62]

Summary

New procedures for synthesizing H_2(pc) and Ni(pc) have led to remarkable improvements in the conductivities of H_2(pc)I and Ni(pc)I. The new materials have $\sigma_{rel}^{max} \sim 30$, corresponding to $\sigma \sim (1$–$2) \times 10^4\ \Omega^{-1}\ cm^{-1}$, at $T \sim 3$ K, whereas all previous studies of charge transport on H_2(pc)I and Ni(pc)I gave $\sigma_{rel}^{max} \lesssim 6$–7 and $T_{max} > 15$ K. The temperature-dependent conductivities for the very pure samples of H_2(pc)I–1 and Ni(pc)I–1 are almost identical, as might be expected because the charge transport occurs through the p–π orbitals of the macrocycle in both cases.

The demonstration that improvement in the purity of the *parent* M(pc) material, M = H_2, Ni, profoundly enhances the low-temperature charge-transport properties of the *product* M(pc)I molecular conductors led to a series of syntheses of the M(pc). H_2(pc)–1 prepared in a melt reaction from pure starting materials in quartz and Teflon containers and then sublimed gave the lowest number of paramagnetic impurities, with <25 ppm of Cu(pc) and <60 ppm of organic radicals ($R^\bullet$). The direct template synthesis of Ni(pc) does not result in high-purity material and is strongly to be discouraged in any application that might suffer from the presence of impurities, e.g. photoconductivity or chemical catalysis. Instead, Ni(pc)–1 with undetectable levels of Cu(pc) (<50 ppm) and ≲200 ppm $R^\bullet$ impurities was prepared by metalation of H_2(pc)–1 and subsequent sublimation. The concentration of radical impurities was not further decreased by additional sublimations.

For $[R^\bullet] \lesssim 300$ ppm, σ_{rel}^{max} *appears* to be independent of $[R^\bullet]$. This suggests that the results represent, for the first time, the *intrinsic* charge-transport properties of H_2(pc)I and Ni(pc)I. The magnetoconductance measurements are consistent with this view. Our work with Cu_xNi_{1-x}(pc)I alloys shows that spin-flip scattering by localized electron spins in fact gives rise to a conductivity maximum, and that T_{max} decreases as the concentration of local moments decreases.[54,55] However, spin-flip scattering in those alloys gave rise to a large positive magnetoconductance for $T \leq T_{max}$,[54] whereas H_2(pc)I–1 and Ni(pc)I–1 show a small negative transverse magnetoconductance for $T \leq T_{max}$, as seen in normal three-dimensional metals.[53] This indicates that the conductivity maximum is not the result of residual paramagnetic metal-ion impurities. Such maxima might also result from spin-density wave, charge-density wave, or anion-ordering phase transitions, which can open a gap at the Fermi surface at temperatures below the transition temperature. However, neither Ni(pc)I–1 nor H_2-

(54) Quirion, G.; Poirier, M.; Liou, K. K.; Hoffman, B. M. *Phys. Rev. B: Condens. Matter* **1991**, *43*, 860–864.
(55) Ogawa, M. Y.; Palmer, S. M.; Liou, K.; Quirion, G.; Thompson, J. A.; Poirier, M.; Hoffman, B. M. *Phys. Rev. B: Condens. Matter* **1989**, *39*, 10682–10692.
(56) Tomkiewicz, Y. *Phys. Rev. B: Solid State* **1979**, *19*, 4038–4048.
(57) Jerome, D.; Schulz, H. J. *Adv. Phys.* **1982**, *31*, 299–490.
(58) Thompson, J. A. Ph.D. Dissertation; Northwestern University: Evanston, Illinois, 1993.
(59) Ferraro, J. R.; Williams, J. M. *Introduction to Synthetic Electrical Conductors*; Academic Press: Orlando, FL, 1987; pp 65–70.
(60) Shiba, H. *Phys. Rev. B: Solid State* **1972**, *6*, 930–938.
(61) Mazumdar, S.; Dixit, S. N. *Phys. Rev. B: Condens. Matter* **1986**, *34*, 3683–3699.
(62) Torrance, J. B.; Tomkiewicz, Y.; Silverman, B. D. *Phys. Rev. B: Solid State* **1977**, *15*, 4738–4749.

(pc)I–1 shows the changes in either the susceptibility or EPR line widths that are expected to accompany such transitions.[56,59] Moreover, if the conductivity maxima observed in H_2(pc)I–1 and Ni(pc)I–1 were due to such a phase transition, this maximum should shift to lower temperature with increasing impurity concentrations, *not* to higher temperature as observed, because disorder tends to suppress such metal → non-metal phase transitions. Examples of this include studies on the effects of radiation-induced defects on the charge-density-wave transition of TTF-TCNQ and the spin-density-wave transition of $[TMTSF]_2[PF_6]$, TMTSF = tetramethyltetraselenafulvalene, which found that the transition temperature decreases with increasing defect concentration for both compounds, as expected.[52,63]

A conductivity maximum, such as seen for H_2(pc)I–1 and Ni(pc)I–1, also can be produced by diamagnetic impurities and defects, which can act as random potentials in quasi-one-dimensional materials and localize the charge carriers at low temperature ("Anderson localization").[47] However, this phenomenon should cause $\sigma \rightarrow 0$ as $T \rightarrow 0$,[47] whereas preliminary conductivity measurements down to 20 mK for H_2(pc)I–1 indicate that this does not occur. This again supports the suggestion that the data reported here reflect *intrinsic* properties of these materials. We are exploring the possibility that the low-temperature properties of H_2(pc)I–1 may represent the phenomenon of "weak localization" in highly anisotropic systems.[64]

Phthalocyanines are widely studied and widely utilized.[5,6] Thus, the development of improved methods for their preparation, such as reported here, may well have wide influences on applications far removed from the present study of quasi-one-dimensional M(pc)I molecular conductors.

Acknowledgment. This work was supported by the Solid State Chemistry Program of the National Science Foundation through Grant No. DMR-9144513 (B.M.H.) and the Northwestern University Materials Research Center, Grant No. DMR-9120521. The EPR analysis software was furnished by the Illinois ESR Research Center, NIH division of Research Resources, Grant No. RR01811. J.A.T. would like to thank Dr. Rama Viswanathan and Clark Davoust for helpful discussions.

Supplementary Material Available: Table IS, additional crystallographic details, and Table IIS, atomic coordinates and anisotropic displacement coefficients (3 pages). Ordering information is given on any current masthead page.

(63) Choi, M.-Y.; Chaikin, P. M.; Huang, S. Z.; Haen, P.; Engler, E. M.; Greene, R. L. *Phys. Rev. B: Condens. Matter* **1982**, *25*, 6208–6217.

(64) Firsov, Y. A. In *Localization and Metal Insulator Transitions*; Fritszsche, H.; Adler, D., Eds.; Plenum: New York, 1985; pp 477–508.